Journal Pre-proofs

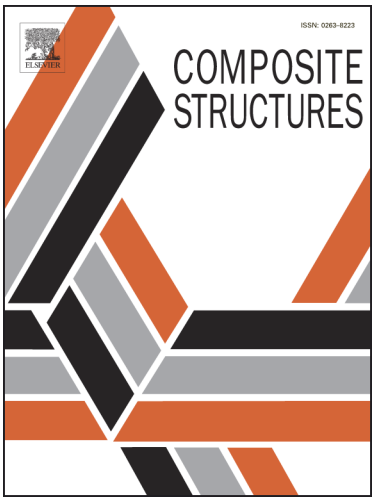

Experimental and analytical investigation on flexural behaviour of RC beams strengthened with NSM CFRP prestressed concrete prisms

Yu Deng, Zhenzhen Li, Hexin Zhang, Alberto Corigliano, Angus C.C. Lam, Chayanon Hansapinyo, Zhitao Yan

PII: S0263-8223(20)33311-0
DOI: https://doi.org/10.1016/j.compstruct.2020.113385
Reference: COST 113385

To appear in: *Composite Structures*

Received Date: 6 June 2020
Revised Date: 17 November 2020
Accepted Date: 21 November 2020

Please cite this article as: Deng, Y., Li, Z., Zhang, H., Corigliano, A., Lam, A.C.C., Hansapinyo, C., Yan, Z., Experimental and analytical investigation on flexural behaviour of RC beams strengthened with NSM CFRP prestressed concrete prisms, *Composite Structures* (2020), doi: https://doi.org/10.1016/j.compstruct.2020.113385

Experimental and analytical investigation on flexural behaviour of RC beams strengthened with NSM CFRP prestressed concrete prisms

Yu Deng[a], Zhenzhen Li[b], Hexin Zhang[c,*], Alberto Corigliano[d], Angus C.C. Lam[e], Chayanon Hansapinyo[f], Zhitao Yan[g]

[a] *School of Civil Engineering and Architecture, Guangxi University of Science and Technology, Liuzhou, China 545006*

[b] *Chalco Shandong Engineering Technology Co., Ltd,Zibo, China 255000*

[c] *School of Engineering and the Built Environment, Edinburgh Napier University, 10 Colinton Road, Edinburgh, Scotland, UK, EH10 5DT*

[d] *Department of Civil and Environmental Engineering, Politecnico di Milano, 20133, Italy*

[e] *Department of Civil and Environmental Engineering, Faculty of Science and Technology, University of Macau, Macau, China*

[f] *Center of Excellence in Natural Disaster Management, Department of Civil Engineering, Chiang Mai University, Chiang Mai, 50200, Thailand*

[g] *School of Civil Engineering, Chongqing University of Science and Technology, Chongqing, China 401331*

Abstract: This investigation aims to study the flexural behaviour of reinforced concrete (RC) beams strengthened with near-surface mounted (NSM) carbon fibre reinforced polymer prestressed concrete prisms (CFRP-PCPs). Eight RC beams were tested under monotonic loading until the failure load was reached. One beam was un-strengthened to act as a control beam. The other seven beams were strengthened with non-prestressed or prestressed NSM CFRP-PCPs. The effects of bond length, prestress level, and concrete type of the CFRP-PCPs on the flexural capacity, flexural crack and deflection are discussed in this paper. The results indicate that the flexural capacity of RC beams strengthened with NSM CFRP-PCPs was greater than the control beam. An obvious improvement was discovered in the crack resistance when the RC beams were strengthened with prestressed

* Corresponding author

E-mail address: j.zhang@napier.ac.uk (Hexin Zhang)

NSM CFRP-PCPs. The strengthened beams showed a higher first-cracking, yielding, and ultimate load as the bond length and prestress level of CFRP-PCPs increased up to a critical level. The beams strengthened with CFRP-PCPs, which were cast with ultra-high performance concrete (UHPC), exhibited greater load capacity than the corresponding beams with epoxy resin mortar. The analytical model of flexural response for the NSM CFRP-PCPs strengthening beams is presented. The analytical results are in good agreement with the experimental results, which revealed the NSM CFRP-PCPs is an effective technique for flexural strengthening of the RC beams.

Keywords: flexural behaviour; NSM strengthening; CFRP-PCPs; analytical model

1. Introduction

Carbon fibre reinforced polymer (CFRP) materials have many advantages including high tensile and fatigue strength, lightweight, strong chemical resistance and non-corroding [1-4]. CFRP materials have been used widely in the field of reinforced concrete (RC) structural strengthening in the past decades due to these excellent enhanced characteristics compared to that of the traditional strengthening materials [5-8]. In general, RC beams strengthened with CFRP composites significantly contributed to enhanced flexural strength, fatigue life and the serviceability of the beams over un-strengthened beams [8-12]. At present, the CFRP strengthening technique for RC structural members includes the externally bonded (EB) strengthening technique and the near-surface mounted (NSM) technique. The NSM CFRP technique has become an effective method for strengthening RC beams, which can significantly improve the flexural performance and stiffness

compared with the EB strengthening technique [6, 8, 13, 14]. Additionally, it shows better durability, fatigue resistance and bonding performance in comparison with the EB CFRP strengthening technique [15, 16].

In construction today, only 20% to 30% of RC beams use the high strength CFRP materials, strengthened with non-prestressed NSM CFRP rods or strips [17]. Non-prestressed strengthened beams fail due to the large deflection and width of crack [18]. As a result, the strengthened beam reaches its ultimate bearing capacity and cannot continue to carry the load. Several studies have attempted to find the most efficient technique to strengthen concrete structures, which led to the combined use of the NSM strengthening method and the prestressing technique (i.e. prestressed NSM technique) [8, 19-23]. In the prestressed NSM technique, the prestressed CFRP rod is usually embedded into grooves cut on the concrete surface and bonded to the concrete with epoxy resin or other adhesives [24-27]. Many researchers have investigated the overall performance of the strengthening RC beams using the prestressed NSM technique. Their results proved that the prestressed CFRP rod can enhance the stiffness, ultimate load, and serviceability limit capabilities of the strengthened RC beams remarkably, in which the prestressed CFRP material was allowed to make full use of its tensile capacity [15, 26, 28-34]. However, it should be noted that there are still some limits in the prestressed NSM technique. For example, the mechanical anchorage system is expensive, prestressing the CFRP rods is a complex process, and there is a high dependency on prestressing equipment [31, 35-39].

Based on existing research and the aforementioned difficulties in the prestressed NSM technique, a new strengthening technique is proposed using NSM carbon fibre reinforced polymer prestressed concrete prisms (CFRP-PCPs), which can improve the performance of the traditional prestressed NSM technique. The NSM CFRP-PCPs technique not only improves the flexural behaviour of strengthened RC beams quite significantly but it also has many other advantages compared with the prestressed NSM CFRP technique. It can be used for shear strengthening as well [40]. The manufacturing method of the CFRP-PCPs will be detailed in Section 2. In this paper, an experimental study was performed to investigate the flexural behaviour of the RC beams strengthened with the NSM CFRP-PCPs. The effects of bond length, prestress level and CFRP-PCPs concrete type on the flexural behaviour of the strengthened beams are discussed. An analytical model for the NSM CFRP-PCPs strengthened RC beams was developed to predict the flexure capacity, deflection and cracking load. This research gives a better understanding of the flexural capacity of the RC beams strengthened with the NSM CFRP-PCPs. Therefore, an appropriate strengthening method can be designed based on the research to utilise the full capacity of the CFRP-PCPs.

2. Experimental procedure

In this section, several aspects of the experimental procedure details are considered including variables of the experiments, test specimens, material properties, strengthening procedure, loading set-up and arrangement of strain gauges, are discussed.

2.1 Variables of the experiments and test specimens

Eight RC beams were designed and tested under static loading using a four-point bending device. In this research, the experimental variables include the bond length, prestress level and concrete type of the CFRP-PCPs. The parameters of all the beams are shown in Table 1.

The overall length and the clear length of the beams were 2600 mm and 2400 mm, respectively. The rectangular cross-section had a depth of 250 mm and a width of 150 mm. All the beams were reinforced in tension, with two 15 mm diameter ribbed steel bars with a steel ratio of 0.96%, and in compression, with two 8 mm diameter ribbed steel bars. The thickness of the concrete cover was 30 mm measured from the external surface of the stirrup to the concrete surface. To prevent shear failure during the loading process, the shear reinforcement consisted of 6 mm diameter ribbed steel stirrups spaced out every 200 mm along the flexural span, while the other stirrups were spaced out every 100 mm along the shear span. The detailed beam dimensions and reinforcement are shown in Fig. 1.

2.2 Material properties

Concrete and steel ribbed bars: All the tested beams and standard cubic concrete blocks (150 mm × 150 mm × 150 mm) were cast with ready mixed concrete and cured in the same condition. The average compressive strength, tensile strength, and modulus of

elasticity of the cubic concrete blocks tested were 30.76 MPa, 3.02 MPa, and 3.27×10^4 MPa, respectively. The steel ribbed bars were tested using standard tensile test methods in [41]. The mechanical properties of the steel ribbed bars are listed in Table 2.

The detailed manufacturing method of the CFRP-PCPs proposed above is as follows:

1) The CFRP rods, 7mm in diameter, were pre-tensioned using the prestressing set-up presented in Fig. 2b; the prestressing level ranged from 30% to 50% of the ultimate capacity of the rods. The prestressing force in the CFRP rod was monitored using strain gauges mounted on the CFRP rod;

2) After pre-tension, the CFRP rods, fixed with the anchors, were placed in the centre of a metal formwork and cast with the ultra-high performance concrete (UHPC) or epoxy resin mortar (Fig 2c). After curing for 15 days to reach the designed strength, the CFRP-PCPs were removed from the prestressing system (Fig 2d);

3) The CFRP-PCPs are the final combined products of the prestressed CFRP rods and the UHPC (Fig 2e). The detailed manufacturing process of the CFRP-PCPs is shown in Fig. 2. The rectangular cross-section of the CFRP-PCPs is 25 mm × 25 mm. The ultimate tensile strength and elastic modulus of the tested CFRP rods were 2400 MPa and 155 GPa, respectively. The standard cubic blocks (70.7 mm × 70.7 mm × 70.7 mm) of the UHPC and

epoxy resin mortar were tested, and the mechanical properties are given in Table 2.

Adhesive: The CFRP-PCPs were inserted into the pre-cut grooves on the concrete surface and bonded to the concrete with the epoxy resin adhesive. The mechanical properties of the epoxy resin, which was provided by the manufacturer (i.e. Liuzhou OVM Machinery Co., Ltd), were 90 MPa in compression and 22.5 MPa in tensile.

2.3 Strengthening procedure

After reaching the designed strength of the concrete, a single groove of 30 mm × 30 mm was cut into the concrete cover on both tensile sides of the beams. The grooves were cleaned to remove fine dust so that strong bonding between the epoxy resin and the CFRP-PCPs could be guaranteed. For the strengthened beams, the groove was half-filled with the epoxy resin and the CFRP-PCPs were then inserted into the groove. The CFRP-PCPs were then gently pressed into the epoxy to make it flow around them. Therefore, good bonding between the adhesive and the CFRP-PCPs was formed. The tested beams were cured for at least one week under a suitable condition to ensure the bond strength.

2.4 Loading set-up and arrangement of strain gauges

All the tested beams were monotonically loaded using a four-point device. The loads were force controlled by the servo-controlled hydraulic jack with the rate of 3 KN/min.

Before the beam cracked, the load increased with each grade of 3 KN. After the cracks appeared, the load increased with each grade of 5 KN until reaching the bending failure load. Five Linear Variable Differential Transducers (LVDT) were located at the mid-span, the loading points and the supports to obtain the vertical deflections. In the mid-span of the beams, several strain gauges were mounted to the steel bars in the tension and compression zone, the CFRP rods and the concrete over the depth of the beams. All the data were collected using a data acquisition system. The crack distribution and the final failure modes were observed. The detailed loading set-up is shown in Fig. 3.

3. Experimental tests and discussion

3.1 Load-deflection relationship

Based on observations of the experimental process, failure modes of the tested beams can be divided into three types. The first type is bending failure which presented in the control beam, JGL2, JGL5, JGL6, and JGL8 beams. The second type is debonding failure which was observed in the JGL3 beam. The beam failed due to peeling that occurred at the boundary between the CFRP-PCPs and the concrete. The third failure mode is epoxy-CFRP rod interface slip failure which occurred in the JGL4 and JGL7 beams. This failure mode was due to the short bond length and poor bonding between the epoxy resin mortar and CFRP rod. The most common failure mode was bending failure, which suggests that the NSM CFRP-PCPs technique is an effective solution to the flexural strengthening of RC beams. Fig.4 shows the failure modes of the tested beams in detail.

3.2 Load-deflection relationship

The load-deflection curves of all the tested beams are shown in Fig. 5. The tested beams exhibited three load-deflection responses: the elastic stage, the yield stage and the ultimate stage. The specific test results are listed in Table 3.

The elastic stage: From initial loading to first cracking of the concrete in the beam bottom, the mid-span deflection of all the tested beams was small and similar to each other because of the strong stiffness of the beam.

The yield stage: From the concrete first cracking to the tensile steel bar yielding, the tensile stress was shared by the CFRP-PCPs and the steel bars together. The cracks continued to expand, and the deflection noticeably increased with a small increase in the external load.

The ultimate stage: From the tensile steel bars yielding to the ultimate load, the stress in the tension zone was mainly carried by the CFRP rods in the NSM CFRP-PCPs. The mid-span deflection of the tested beams increased rapidly and the external load decreased when the beams reached the ultimate stage.

Table 3 presents the cracking load, yield load and ultimate load of the tested beams. The control beam performance was 13.18 KN, 64.98 KN and 69.72 KN, respectively. In comparison to the control beam, the cracking load, yield load and ultimate load of the non-prestressed strengthened beam (JGL2) increased by 24.96%, 36.01%, and 56.91%, respectively. For the 30% prestressed strengthened beam (JGL6), a significant increase of

37.48%, 60.55% and 67.98% was obtained in the cracking load, yield load and ultimate load, respectively. The cracking load of the 50% prestressed strengthened beam (JGL8) was higher than that of 30% prestressed strengthened beam. However, the prestress level had little effect on the ultimate load for the strengthened beams, as seen by comparing beams JGL2, JGL6 and JGL8. The ultimate load for JGL6 (bond length of 2000 mm) was 116.36 KN, showing a 67.98% increase over that of the control beam and a 56.8% increase over the JGL3 beam (bond length of 1000 mm). Therefore, the ultimate load increased as the bond length of the CFRP-PCPs increased. The ultimate deflection of beams JGL2, JGL6 and JGL8 were 39.2 mm, 36.33 mm and 33 mm, respectively. The difference in deflection in prestressed strengthened beams indicates that deflection decreases with the increasing prestress levels.

According to the test results, the effective length of the CFRP-PCPs is 1800 mm to 2200 mm. Comparative of the results of beams JGL7 and JGL8 illustrates that the ultimate load of the strengthened beams using the CFRP-PCPs which were cast with the UHPC was higher than those with the epoxy resin mortar. Additionally, the application of prestressed CFRP-PCPs can improve the cracking load capacity as well as significantly reduce mid-span deflection of the strengthened beams.

3.3 Ductility

The definition of curvature ductility was the ratio of the ultimate curvature to yield curvature. The curvature ductility of the control beam, the beams JGL2, JGL6 and JGL8

were 10.62, 4.36, 3.54, 2.65, respectively. In comparison with the control beam, the curvature ductility of the beams JGL2, JGL6, and JGL8 was decreased by 58.9%, 66.6%, 75%, respectively. The prestressing force of the CFRP-PCPs can produce a negative bending moment to reduce the mid-span deflection and the cracked portion of the beam cross-section. However, the prestressing force also resulted in a decrease in the energy dissipation, which led to a decrease in the curvature ductility as well.

3.4 Load-strain relationship

Fig. 6 displays the load-strain curves in the compressed concrete, the CFRP rods and the tensile steel bars during the loading process. As shown in Fig. 6a, the compressive strain in the tested beams increased with a greater external load. In fact, the prestressing force in the prestressed strengthened beam can create the initial tensile stress in the beam-top concrete. Therefore, the depth of the compression zone was higher than the control beam and the non-prestressed strengthened beam. Beam JGL8 showed less compressive strain at the top fibre of cross-section than control beam under the same load. The control beam, L1, and beam JGL2 failed due to crushing in the beam-top concrete at a maximum concrete compression strain of about 4900 με and 3990 με, respectively. Beams JGL6 and JGL8 had smaller ultimate compressive strains of about 2800 με and 1450 με, respectively. Therefore, the prestressing force induced the initial tensile strains, which could reduce the compressive strains at failure for the prestressed strengthened beams.

Fig. 6b represents the load-strain curves of the CFRP rods for beams JGL2, JGL6 and JGL8. The strain induced by the prestressing force of the CFRP rods was not considered. CFRP rod strain increased with an increasing external load. The slope of the load-strain curves for the three beams was similar before the cracking of the bottom concrete. After the presence of the crack in the beam concrete, the strain of non-prestressed beam significantly increased over that of the 30% and 50% prestressed beams in the same load. The application of prestressed CFRP-PCPs inhibited the development of cracks and improved the stiffness of beams more effectively compared to that of the non-prestressed strengthened beam.

Fig. 6c shows the load-strain curves of the tensile steel bars. The control beam had a larger strain in the tensile steel bars under the corresponding loads compared to that of beam JGL2 and beam JGL6. In the 0% and 30% prestressed strengthened beams, the external load was shared by the tensile steel bars and the CFRP-PCPs. Using CFRP-PCPs reduced the tensile stress in the tension reinforcement, which resulted in the ultimate load of beams JGL2 and JGL6 being higher than that of the control beam.

4. The analytical model

4.1 Basic assumptions

An analytical model was proposed for calculating the flexural capacity, cracking load, and deflection of RC beams strengthened with the NSM CFRP-PCPs. The basic assumptions in the model are as follows:

1) During the loading process, the tested beams strengthened with the NSM CFRP-PCPs conform to the assumption of a plane section.

2) The tensile strength of concrete is not considered after cracking.

3) The stress-strain curves of internal steel bars can be simplified to an ideal elastic-plasticity. The CFRP rod has a linear elastic stress-strain relationship up to failure. $\varepsilon_{s,\,max}$ is the ultimate tensile strain of steel bars and $\varepsilon_{s,\,max}$=0.01.

4) The model of concrete in compression can be expressed by the following equations:

$$f_c = f_c^{'}\left[1-(1-\frac{\varepsilon_c}{\varepsilon_0})^2\right] \qquad 0 < \varepsilon_c \le \varepsilon_0 \qquad 1(a)$$

$$f_c = f_c^{'} \qquad \varepsilon_0 < \varepsilon_c \le \varepsilon_{cu} \qquad 1(b)$$

Where f_c is the concrete compressive stress corresponding to a given strain (ε_c), $f_c^{'}$ is the cylinder compressive strength of concrete, ε_c is the compressive strain of concrete, ε_0 is the compressive strain of concrete at the peak stress and ε_0=0.002, ε_{cu} is the ultimate strain of compression concrete and ε_{cu}=0.003.

5) The bond between the concrete, the steel bars and the two bonding interfaces (CFRP-PCPs and concrete-epoxy) is perfect.

4.2 Calculation for flexural strength capacity

4.2.1 The balanced condition

For the tested beams strengthened with the NSM CFRP-PCPs, the balanced condition is when the tensile strain in the prestressed CFRP rods reaches to its ultimate tensile limitation just as the concrete in compression reaches its assumed ultimate strain of 0.003

[18]. By this time, the tensile steel bars have already reached their ultimate strength. Fig. 7 shows the distribution of stress and strain across the depth of the rectangular cross-section under the balanced condition.

According to the force equilibrium and strain compatibility requirements, the equation can be expressed as follows:

$$x_{cb} = \frac{\varepsilon_{cu}}{\varepsilon_{cu} + \varepsilon_{fu}} h_f \tag{2}$$

$$\alpha_1 f_c b x_b + f_y^{'} A_s^{'} - f_y A_s - f_{fu} A_{fb} = 0 \tag{3}$$

With

$$x_b = \beta_1 x_{cb} \tag{4}$$

$$f_f = \varepsilon_f E_f \tag{5}$$

The area of CFRP rods under the balanced condition can be solved from Eqs. (2) and (3):

$$A_{fb} = \frac{\alpha_1 f_c b x_b + f_y^{'} A_s^{'} - f_y A_s}{f_{fu}} \tag{6}$$

Where x_{cb} is the actual depth of the neutral axis in cross-section under the balanced condition, x_b is the depth of the equivalent rectangular compression stress block , A_s is the area of the tensile steel bar, $A_s^{'}$ is the area of the compression steel bar, A_{fb} is the balanced area of the CFRP rod, b is the width of the rectangular beam cross-section, h_f is the distance from the centre of CFRP rod to the beam top, α_1 is the ratio of the equivalent stress in the compression stress block to the concrete strength and $\alpha_1 = 1$, β_1 is the ratio of the depth of the compression stress block to the fibre depth of the neutral axis and $\beta_1 = 0.8$, f_f and f_{fu} are the stress and ultimate stress $(f_{fu} = 2200Mpa)$ of the CFRP rod, f_y is the

yield strength of the tensile steel bars, $f_y^{'}$ is the yield strength of the compressive steel bars, E_f is the elastic modulus of the CFRP rod, ε_{cu} is the ultimate strain of compression concrete and ε_{cu}=0.003. ε_f and ε_{f_u} are the strain and ultimate strain($\varepsilon_{f_u}=0.014$) in the CFRP rod, respectively.

If the area of the CFRP rod (A_f) is below a balanced value A_{fb} or the depth of the equivalent rectangular concrete stress block x is below x_b, the rupture of CFRP rods (i.e., tension failure) will occurs prior concrete crushing. If $A_f > A_{fb}$ or $x > x_b$, the strengthened beams will fail by concrete crushing in compression zone (i.e., compression failure).

4.2.2 Tension failure

The nature of tension failure means that the CFRP rods will rupture before the compressive concrete is crushed. The distribution of stress and strain across the depth of the section in tension failure mode is presented in Fig. 8. According to the maximum compressive strain of the beam-top concrete, the tension failure mode can be divided into two cases. The compressive strain of concrete does not reach the ultimate strain of compression concrete, ε_{cu}. Hence, the compressive stress of concrete cannot be calculated according to the equivalent rectangular stress specified in ACI 318-19 [42]. Referring to the calculated methods in [43], the following equations can be obtained:

Case 1: $0 < \varepsilon_c \le \varepsilon_0$

$$C_c = \left(\frac{\varepsilon_c}{\varepsilon_0} - \frac{\varepsilon_c^2}{3\varepsilon_0^2} \right) f_c b x_c \tag{7}$$

$$y_c = \frac{4\varepsilon_0 - \varepsilon_c}{12\varepsilon_0 - 4\varepsilon_c} x_c \tag{8}$$

Case 2: $\varepsilon_0 < \varepsilon_c \le \varepsilon_{cu}$

$$C_c = \left(1 - \frac{\varepsilon_c}{3\varepsilon_0}\right) f_c b x_c \tag{9}$$

$$y_c = 1 - \frac{3 - \frac{\varepsilon_0^{\,2}}{2\varepsilon_c^{\,2}}}{6 - 2\frac{\varepsilon_0}{\varepsilon_c}} x_c \tag{10}$$

Where C_c is the compressive force of concrete, x_c is the actual depth of the neutral axis in cross-section， y_c is the distance from the centroid of the concrete compressive force to the beam-top edge of the concrete compressive zone, ε_c is the compressive strain of concrete, ε_0 is the compressive strain of concrete at the peak stress and ε_0=0.002. Based on the strain compatibility and the equilibrium of forces, the following equation can be obtained:

$$\varepsilon_c = \frac{x_c}{h_f - x_c} \varepsilon_{fu} \tag{11}$$

$$\varepsilon_s^{'} = \frac{x_c - a_s^{'}}{h_f - x_c} \varepsilon_{fu} \tag{12}$$

$$C_c + E_s \varepsilon_s^{'} A_s^{'} = f_y A_s + f_{fu} A_f \tag{13}$$

The ultimate moment capacity of the strengthened beam under tension failure can be solved from Eqs. (7) - (13), and expressed as the following:

$$M_u = E_s \varepsilon_s^{'} A_s^{'} (a_s^{'} - y_c) + f_u A_s (h_0 - y_c) + f_{fu} A_f (h_f - y_c) \tag{14}$$

Where E_s is the elastic modulus of the steel bars, $\varepsilon_s^{'}$ is the strain in the compressive steel

reinforcement, and A_f is the section area of the CFRP rod.

4.2.3 Compression failure

The strengthened beams will fail due to the concrete crushing in compression zone before the rupture of CFRP rods (i.e. $\varepsilon_f < \varepsilon_{fu}$) when $A_f > A_{fb}$ or $x > x_b$. The compression failure mode can be divided into two cases depending on whether the tensile steel bars yield or not. Fig. 9 shows the distribution of stress and strain across the strengthened section under compression failure. The CFRP-PCPs developed several cracks during the loading process. Therefore, it is assumed that the corresponding load was transferred to the CFRP rods. Based on this assumption, the following equation can be obtained:

$$T_p = \sigma_{pe} A_f + f_p A_0 \tag{15}$$

Where T_p is the required load corresponding to the rupture of the CFRP-PCPs, σ_{pe} is the effective stress in the CFRP rod due to the initial prestress, f_p is the tensile strength of the UHPC, and A_0 is the effective area of the CFRP-PCPs.

Based on the compatibility of strain and the equilibrium of internal forces, the following equations can be obtained:

Case 3: $\varepsilon_s \geq \varepsilon_y, \varepsilon_f < \varepsilon_{fu}, \varepsilon_c = \varepsilon_{cu}$

$$\varepsilon_f = \frac{\beta_1 h_f - x}{x}\varepsilon_{cu} \tag{16}$$

$$\varepsilon_s^{'} = \frac{x - \beta_1 a_s^{'}}{x}\varepsilon_{cu} \tag{17}$$

$$\alpha_1 f_c b x + E_s \varepsilon_s^{'} A_s^{'} = f_y A_s + f_f A_f + T_p \tag{18}$$

Case 4: $\varepsilon_s < \varepsilon_y, \varepsilon_f < \varepsilon_{fu}, \varepsilon_c = \varepsilon_{cu}$

$$\varepsilon_s = \frac{\beta_1 h_0 - x}{x}\varepsilon_{cu} \tag{19}$$

$$\alpha_1 f_c b x + E_s \varepsilon_s^{'} A_s^{'} = E_s \varepsilon_s A_s + f_f A_f + T_p \tag{20}$$

With $x = \beta_1 x_c$

The equations of ε_f and $\varepsilon_s^{'}$ in this case are the same as those in Case 3. x, in Cases 3 and 4, can be solved from Eqs. (15) - (20).

The ultimate bearing capacity of the strengthened beams under compression failure can be calculated by the following equation:

$$M_u = \alpha_1 f_c b x (h_0 - \frac{x}{2}) + \sigma_s^{'} A_s^{'} (h_0 - a_s^{'}) - \left(f_f A_f + T_p\right)\left(h_0 - h_f\right) \tag{21}$$

4.3 Calculation for cracking capacity

The cracking capacity of RC strengthened beams can be calculated by modifying the elastic modulus of pre-stressed CFRP-PCPs. The specific formulas are as follows:

$$E_p^{'} = \frac{f_p + \sigma_{pe}}{\varepsilon_p} = \frac{\left(f_p + \sigma_{pe}\right)}{f_p} E_p \tag{22}$$

$$I_0 = \frac{b}{3}\left[x_0^{\,3} + (h - x_0)^3 \right] + (n_s - 1)A_s^{'}(x_0 - a_s^{'})^2 + (n_s - 1)A_s(h_0 - x_0)^2$$

$$+(n_p - 1)A_p(h_f - x_0)^2 + (n_f - 1)A_f(h_f - x_0)^2 \quad (23)$$

$$W_0 = I_0 / \left(h - x_0\right) \quad (24)$$

The cracking moment of the strengthened beam can be solved from Eqs. (22) - (24):

$$M_{cr} = \gamma W_0 f_t \quad (25)$$

With $\gamma = (0.7 + 120/h)\gamma_m$ (26)

The mid-span external load (P_{cr}) can be calculated as follows:

$$P_{cr} = \frac{2M_{cr}}{a} \quad (27)$$

Where x_0 is the depth of the neutral axis in a composite section considering the steel and CFRP-PCPs, a is the shear span length of strengthened beams and M_{cr} is the cracking moment of the strengthened beam. $E_p^{'} / E_c = n_p, E_s / E_c = n_s, E_f / E_c = n_f$, where $E_p^{'}$ is the correction elastic modulus of the UHPC in CFRP-PCPs considering the prestressing force, E_f is the elastic modulus of the CFRP rod, and E_s is the elastic modulus of the steel bar. A_p is the effective area of CFRP-PCPs after deducting the area of the CFRP rods, I_0 is the section moment of inertia when considering the contribution of the CFRP-PCPs, W_0 is the section modulus of tension fibre in the bottom of the beam, γ is the plastic coefficients of section modulus and γ_m=1.55.

4.4 Calculation for deflection

For the un-cracked beams, the mid-span elastic deflection can be calculated by the usual methods with a constant value of $E_c I_0$ along the length of beams. However, if the beams crack at one or more sections, the softening effect of cracks on beams should be considered in the calculation. After the crack appeared in the tested beams, the effective moment of inertia, I_{eff} developed in ACI 318-08, can be used in the deflection calculation. Also, Tadros M.K. et al. proposed that the effect of the initial curvature due to prestressing on the members should be taken seriously [44]. Therefore, the effective moment of inertia can be obtained by the following formula:

$$I_{eff} = \left(\frac{M_{cr} - M_{dc}}{M - M_{dc}} \right)^3 I_0 + \left[1 - \left(\frac{M_{cr} - M_{dc}}{M - M_{dc}} \right)^3 \right] I_{cr} \le I_0 \tag{28}$$

Where M_{cr} is the flexural cracking moment considering the prestressed CFRP-PCPs, M_{dc} is the decompression moment, which represents the state at which the initial compression stress in the concrete is nullified to zero stress by the externally applied load, M is the maximum moment in the beam at which the deflection is being computed, I_{cr} is the cracked moment of inertia and I_{cr} can be solved from Eqs. (29) - (30):

$$\frac{1}{2} b x_{cr}^{\ 2} + n_s A_s^{'} (x_{cr} - a_s^{'}) = n_s A_s (h_0 - x_{cr}) + n_f A_f (h_f - x_{cr}) \tag{29}$$

$$I_{cr} = \frac{b}{3} x_{cr}^{\ 3} + n_s A_s^{'} (x_{cr} - a_s^{'})^2 + n_s A_s (h_0 - x_{cr})^2 + n_f A_f (h_f - x_{cr})^2 \tag{30}$$

Where x_{cr} is the depth of the neutral axis of the cracked section, considering the contribution of the steel bars and the CFRP rods. After the strengthened beams crack, the deflection can be calculated using the structural mechanics method with the effective moment of inertia I_{cr}.

5. Verification of the analytical model

This section compares the experimental results with the mechanical behaviour predictions of the RC beams strengthened with prestressed CFRP-PCPs using the analytical model.

5.1 Flexural capacity

The analytical results for the flexural capacity of the strengthened beams are compared with the experimental results and are listed in Table 4. The analytical flexural ultimate load agrees well with the experimental results.

5.2 Cracking load

Table 5 shows excellent agreement between the analytical model and experimental results for the cracking load in the tested beams. The predicted value of the cracking load can be calculated by Eq. (27). As shown in Table 5, the analytical model is relatively accurate and can reliably predict the cracking load of the flexural strengthening beams.

5.3 Load-deflection

The deflection of tested beams under the yield load could be calculated by the analytical model using the effective moment of inertia. The predicted deflections of the flexural beams are listed in Table 6 and compared with the experimental values. It can be observed that the predicted deflections agree well with the experimental results.

6. Conclusions

1) This paper presents an experimental study that aims to use CFRP-PCPs with NSM to strengthen the reinforced concrete beam flexural stiffness and enhance performance. The experiment itself and the result have demonstrated that the proposed technique is an effective and construction-friendly practical method for strengthening concrete beams.

2) The prestressed force inside CFRP-PCPs has restrained the crack propagation and reduced the crack width. However, it also noticed that the ductility of the strengthened beams was decreased.

3) The test results also reveal that the NSM CFRP-PCPs strengthen beams have achieved a considerable increase in bending capacity and decrease in mid-span deflection compared to the control beam. The cracking load increased significantly when the bond length and prestress level increased. The CFRP-PCPs cast with the UHPC performed better than those cast with the epoxy resin mortar.

4) The ductility of the beams decreased as the level of prestressing in CFRP-PCPs

increased. If the CFRP rod used were prestressed to 30% of its ultimate load, the ductility of the strengthened beam reduced by 66%.

5) The analytical model was developed to predict the capacity, stiffness and deflection of the NSM CFRP-PCPs strengthened concrete beams. The analytical results agreed well with the experimental results.

Acknowledgements

The authors gratefully acknowledge the financial support of the National Nature Science Foundation of China (51768008), British Council and Ministry of Education, China (UK-China-BRI Countries Education Partnership Initiative 2019), China Postdoctoral Science Foundation Project (2017M613273XB), Liuzhou Scientific Research and Technology Development Plan (2017BC40202), Nature Science Foundation of Guangxi Zhuang Autonomous Region (2019JJA160137) and Royal Academy of Engineering – Industrial Fellowship (IF\192023). The authors also acknowledge the support of Innovation Team Support Plan of Guangxi University of Science and Technology.

References

1. Aslam, M., et al., *Strengthening of RC beams using prestressed fiber reinforced polymers - A review.* Construction and Building Materials, 2015. **82**: p. 235-256.
2. Afefy, H.M., K. Sennah, and H. Akhlagh-Nejat, *Experimental and analytical investigations on the flexural behavior of CFRP-strengthened composite girders.* Journal of Constructional Steel Research, 2016. **120**: p. 94-105.

3. El-Hacha, R. and K. Soudki, *Prestressed near-surface mounted fibre reinforced polymer reinforcement for concrete structures - A review.* Canadian Journal of Civil Engineering, 2013. **40**(11): p. 1127-1139.
4. Teng, J.G., T. Yu, and D. Fernando, *Strengthening of steel structures with fiber-reinforced polymer composites.* Journal of Constructional Steel Research, 2012. **78**: p. 131-143.
5. Narmashiri, K., M.Z. Jumaat, and N.H.R. Sulong, *Shear strengthening of steel I-beams by using CFRP strips.* Scientific Research and Essays, 2010. **5**(16): p. 2155-2168.
6. Rahal, K.N. and H.A. Rumaih, *Tests on reinforced concrete beams strengthened in shear using near surface mounted CFRP and steel bars.* Engineering Structures, 2011. **33**(1): p. 53-62.
7. Hawileh, R.A., et al., *Behavior of reinforced concrete beams strengthened with externally bonded hybrid fiber reinforced polymer systems.* Materials & Design, 2014. **53**: p. 972-982.
8. Sharaky, I.A., L. Torres, and H.E.M. Sallam, *Experimental and analytical investigation into the flexural performance of RC beams with partially and fully bonded NSM FRP bars/strips.* Composite Structures, 2015. **122**: p. 113-126.
9. Al-Mahmoud, F., et al., *Strengthening of RC members with near-surface mounted CFRP rods.* Composite Structures, 2009. **91**(2): p. 138-147.
10. Attari, N., S. Amziane, and M. Chemrouk, *Flexural strengthening of concrete beams using CFRP, GFRP and hybrid FRP sheets.* Construction and Building Materials, 2012. **37**: p. 746-757.
11. Elsanadedy, H.M., et al., *Flexural strengthening of RC beams using textile reinforced mortar - Experimental and numerical study.* Composite Structures, 2013. **97**: p. 40-55.
12. Zhu, Z., et al., *Flexural fatigue behavior of large-scale beams strengthened with side near surface mounted (SNSM) CFRP strips.* Engineering Structures, 2019. **180**: p. 134-147.
13. Haddad, R.H. and O.A. Almomani, *Flexural performance and failure modes of NSM*

CFRP-strengthened concrete beams: A parametric study. International Journal of Civil Engineering, 2019. **17**(7A): p. 935-948.

14. Sharaky, I.A., et al., *Flexural response of reinforced concrete (RC) beams strengthened with near surface mounted (NSM) fibre reinforced polymer (FRP) bars.* Composite Structures, 2014. **109**(2014): p. 8-22.
15. Badawi, M. and K. Soudki, *Flexural strengthening of RC beams with prestressed NSM CFRP rods - Experimental and analytical investigation.* Construction and Building Materials, 2009. **23**(10): p. 3292-3300.
16. Barros, J.A.O., I.G. Costa, and A. Ventura-Gouveia, *CFRP Flexural and Shear Strengthening Technique for RC Beams: Experimental and Numerical Research.* Advances in Structural Engineering, 2011. **14**(3): p. 551-573.
17. Yang, D.-S., S.-K. Park, and K.W. Neale, *Flexural behaviour of reinforced concrete beams strengthened with prestressed carbon composites.* Composite Structures, 2009. **88**(4): p. 497-508.
18. Xue, W.C., Y. Tan, and L. Zeng, *Flexural response predictions of reinforced concrete beams strengthened with prestressed CFRP plates.* Composite Structures, 2010. **92**(3): p. 612-622.
19. Motavalli, M., C. Czaderski, and K. Pfyl-Lang, *Prestressed CFRP for strengthening of reinforced concrete structures: Recent developments at Empa, Switzerland.* Journal of Composites for Construction, 2011. **15**(2): p. 194-205.
20. Peng, H., et al., *An experimental study on reinforced concrete beams strengthened with prestressed near surface mounted CFRP strips.* Engineering Structures, 2014. **79**: p. 222-233.
21. Wahab, N., K.A. Soudki, and T. Topper, *Experimental investigation of bond fatigue behavior of concrete beams strengthened with NSM prestressed CFRP rods.* Journal of Composites for Construction, 2012. **16**(6): p. 684-692.
22. Oudah, F. and R. El-Hacha, *Fatigue behavior of RC beams strengthened with prestressed NSM CFRP rods.* Composite Structures, 2012. **94**(4): p. 1333-1342.

23. Ye, Y., Z.X. Guo, and Z.L. Chai, *Flexural behavior of stone slabs reinforced with prestressed NSM CFRP bars.* Journal of Composites for Construction, 2014. **18**(4).
24. Si-Larbi, A., et al., *Strengthening RC beams with composite fiber cement plate reinforced by prestressed FRP rods: Experimental and numerical analysis.* Composite Structures, 2012. **94**(3): p. 830-838.
25. Hong, S. and S.-K. Park, *Effect of prestress and transverse grooves on reinforced concrete beams prestressed with near-surface-mounted carbon fiber-reinforced polymer plates.* Composites Part B-Engineering, 2016. **91**: p. 640-650.
26. Alcaraz Carrillo de Albornoz, V., et al., *Experimental study of a new strengthening technique of RC beams using prestressed NSM CFRP bars.* Sustainability, 2019. **11**(5).
27. Rezazadeh, M., I. Costa, and J. Barros, *Influence of prestress level on NSM CFRP laminates for the flexural strengthening of RC beams.* Composite Structures, 2014. **116**: p. 489-500.
28. Lee, H.Y., W.T. Jung, and W. Chung, *Flexural strengthening of reinforced concrete beams with pre-stressed near surface mounted CFRP systems.* Composite Structures, 2017. **163**: p. 1-12.
29. Choi, H.T., J.S. West, and K.A. Soudki, *Effect of partial unbonding on prestressed near-surface-mounted CFRP-strengthened concrete T-beams.* Journal of Composites for Construction, 2011. **15**(1): p. 93-102.
30. Kara, I.F., A.F. Ashour, and M.A. Koroglu, *Flexural performance of reinforced concrete beams strengthened with prestressed near-surface-mounted FRP reinforcements.* Composites Part B-Engineering, 2016. **91**: p. 371-383.
31. Liang, J.F., et al., *Flexural behaviour of reinforced concrete beams strengthened with NSM CFRP prestressed prisms.* Structural Engineering and Mechanics, 2017. **62**(3): p. 291-295.
32. Rezazadeh, M., J. Barros, and I. Costa, *Analytical approach for the flexural analysis of RC beams strengthened with prestressed CFRP.* Composites Part B-Engineering, 2015. **73**: p. 16-34.

33. Omran, H.Y. and R. El-Hacha, *Nonlinear 3D finite element modeling of RC beams strengthened with prestressed NSM-CFRP strips.* Construction and Building Materials, 2012. **31**: p. 74-85.
34. Zhu, Z. and E. Zhu, *Flexural behavior of large-size RC beams strengthened with side near surface mounted (SNSM) CFRP strips.* Composite Structures, 2018. **201**: p. 178-192.
35. Nilimaa, J., et al., *NSM CFRP strengthening and failure loading of a posttensioned concrete bridge.* Journal of Composites for Construction, 2016. **20**(3).
36. Kim, Y.J., J.-Y. Kang, and J.-S. Park, *Post-tensioned NSM CFRP strips for strengthening PC beams: A numerical investigation.* Engineering Structures, 2015. **105**: p. 37-47.
37. Jung, W.-t., et al., *Flexural behaviour of RC beams strengthened with prestressed CFRP NSM tendon using new prestressing system.* International Journal of Polymer Science, 2017.
38. Oudah, F. and R. El-Hacha, *Analytical fatigue prediction model of RC beams strengthened in flexure using prestressed FRP reinforcement.* Engineering Structures, 2013. **46**: p. 173-183.
39. Park, H.B., et al., *Fatigue behavior of concrete beam with prestressed near-surface mounted CFRP reinforcement according to the strength and developed length.* Materials, 2019. **12**(1): p. 15.
40. Deng, Y., et al., *Experimental Study on Shear Performance of RC Beams Strengthened with NSM CFRP Prestressed Concrete Prisms* Engineering Structures, 2020. Accepted.
41. E8M-16ae1, A.E., *Standard Test Methods for Tension Testing of Metallic Materials*, in *ASTM International, West Conshohocken, PA*. 2016: ASTM International, West Conshohocken, PA.
42. 318, A.C., *318-19: Building Code Requirements for Structural Concrete and Commentary*. 2019: American Concrete Institute. p. 624.
43. Wang, W.W., *Technology and application of FRP reinforcing concrete structures*.

2007: China Construction Industry Press.

44. Tadros, M.K., A. Ghali, and A.W. Meyer, *Prestressed loss and deflection of precast concrete members.* Pci Journal, 1985. **30**(1): p. 114-141.

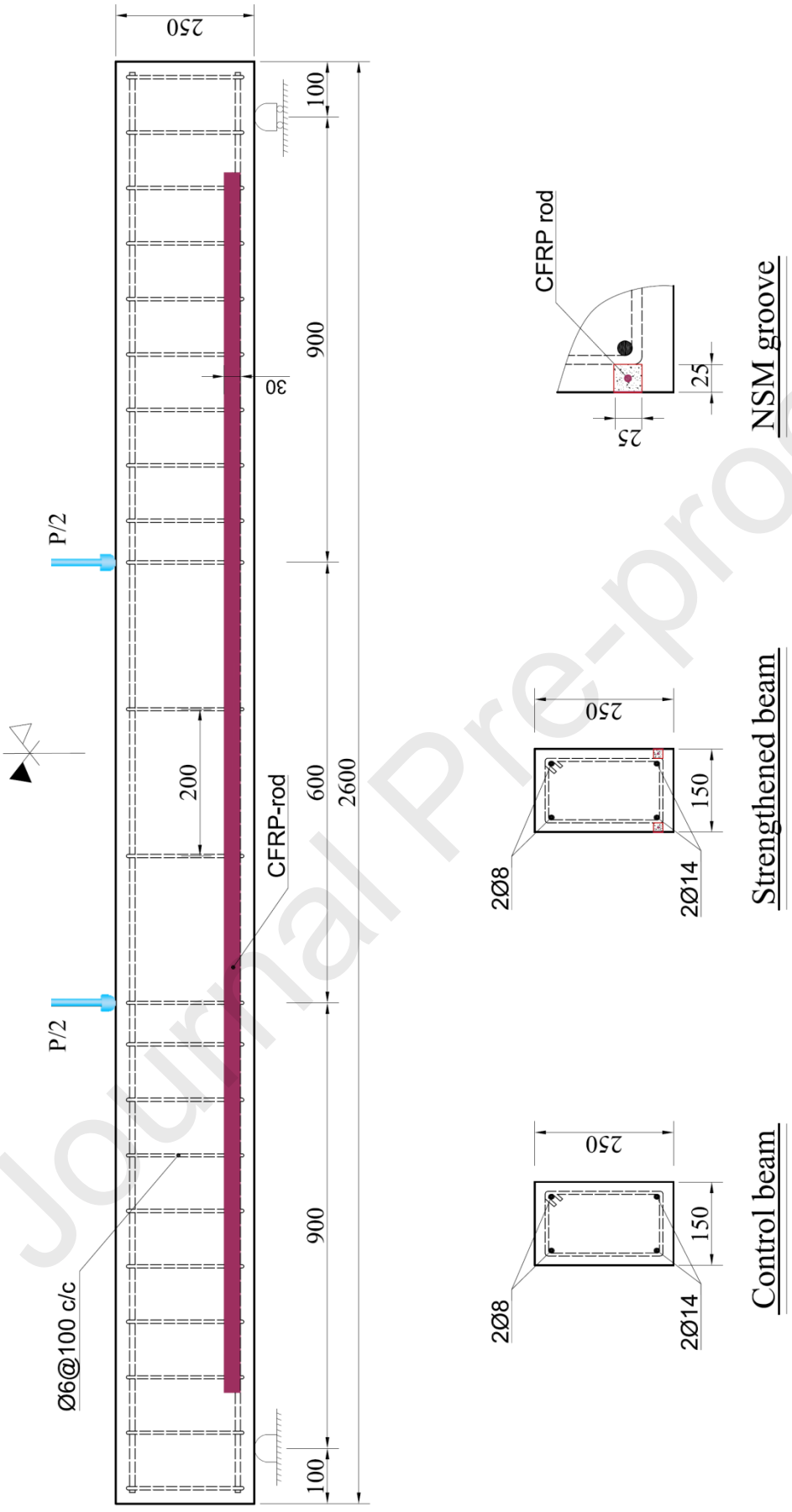

Fig. 1. Dimensions and reinforcement of beam specimen

a) Installation of CFRP rods.

b) Prestressing the CFRP rods.

c) Pouring the concrete.

d) Curing of the CFRP-PCPs.

e) The finished CFRP-PCPs.

Fig. 2. The manufacturing process of the CFRP-PCPs.

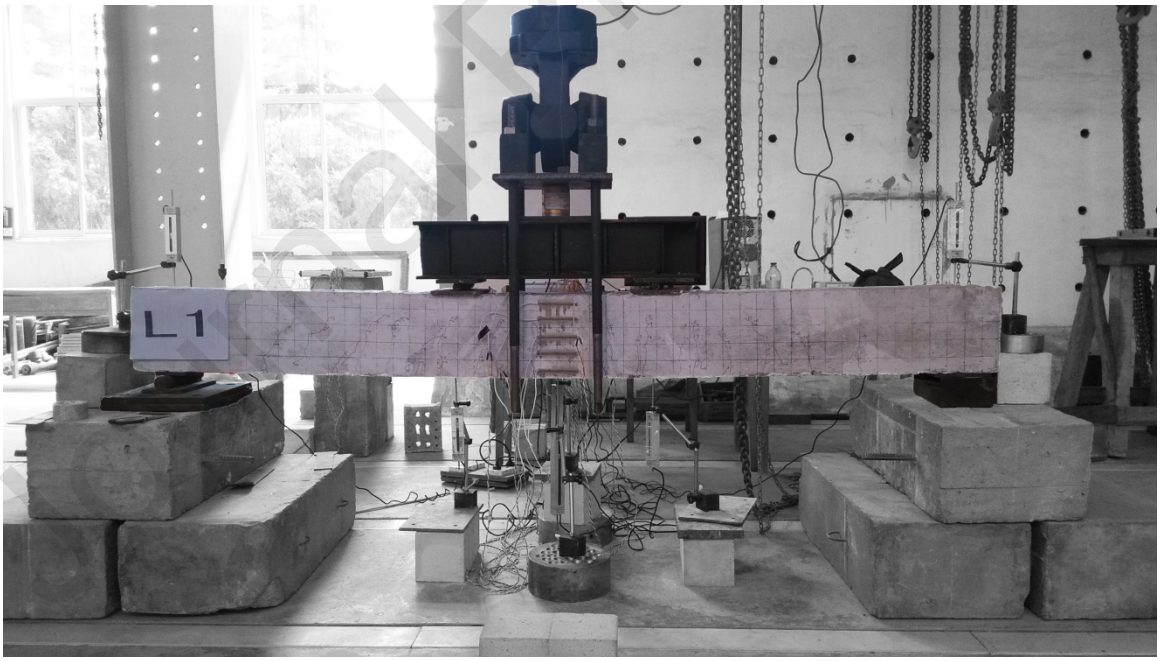

Fig. 3. Loading set-up

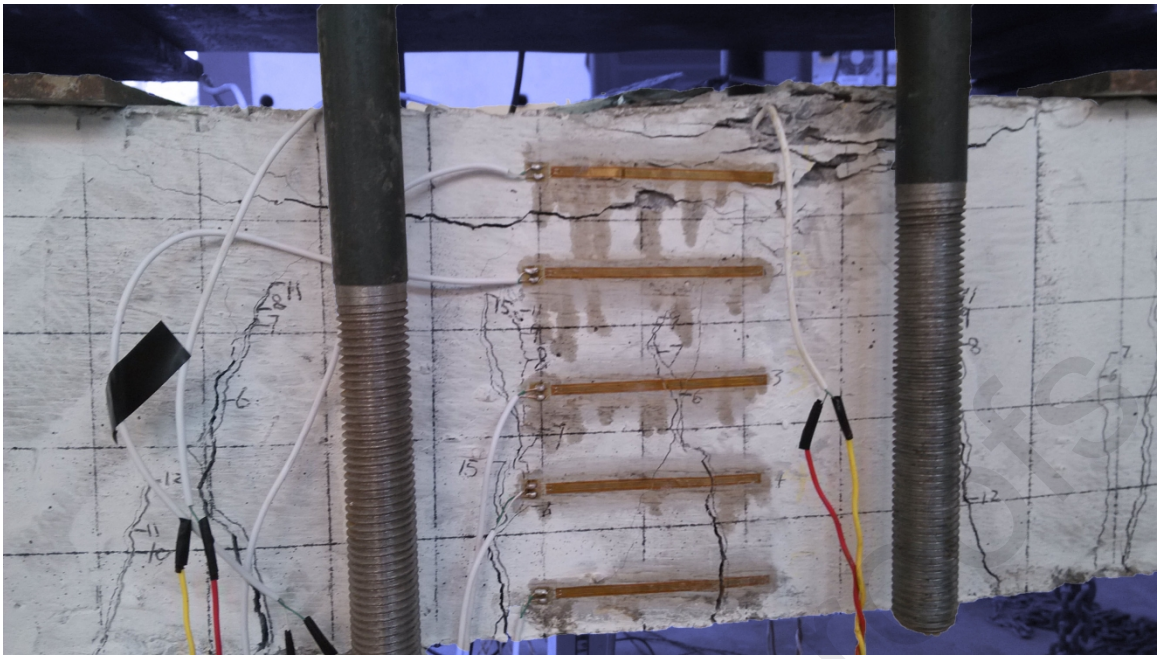

a) Beam L1

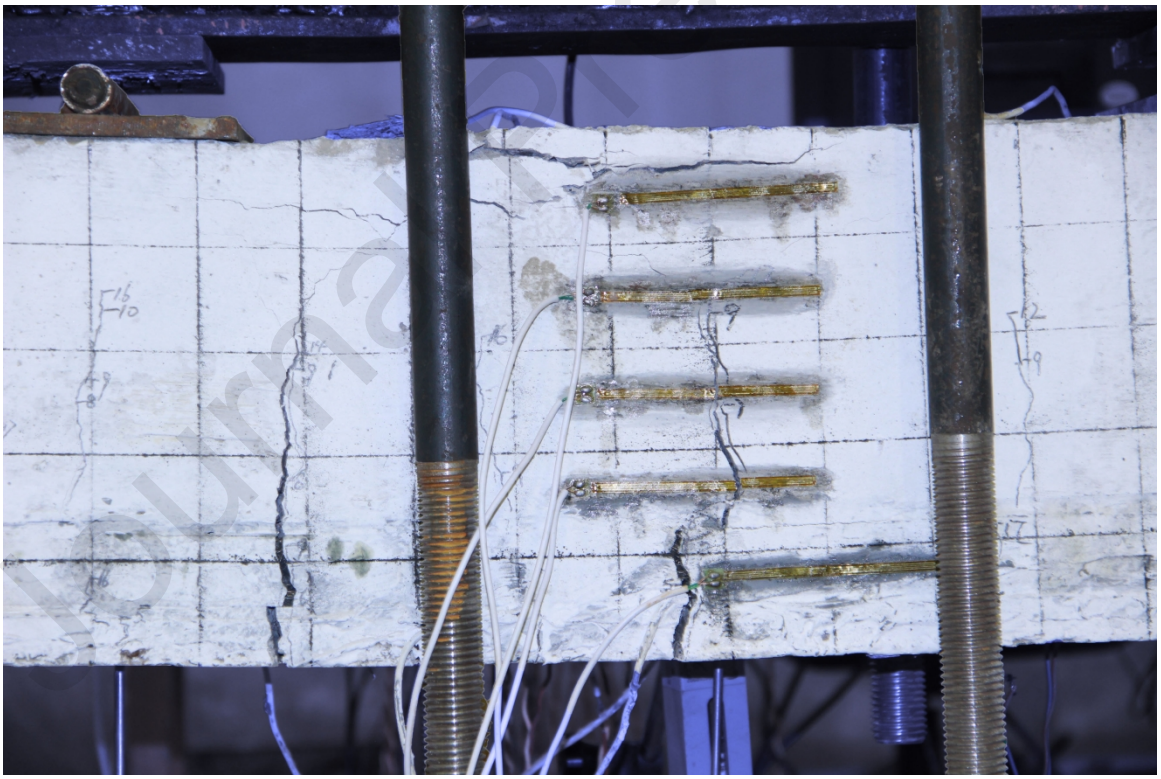

b) Beam JGL2

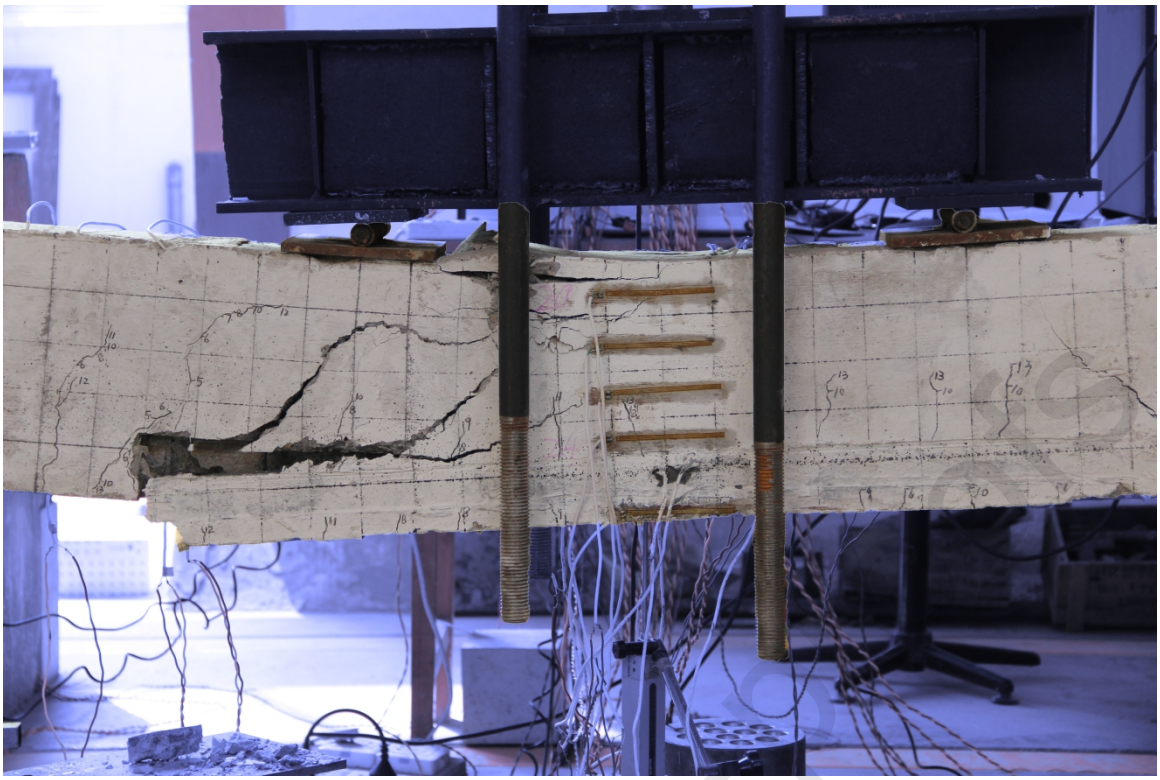

c) Beam JGL3

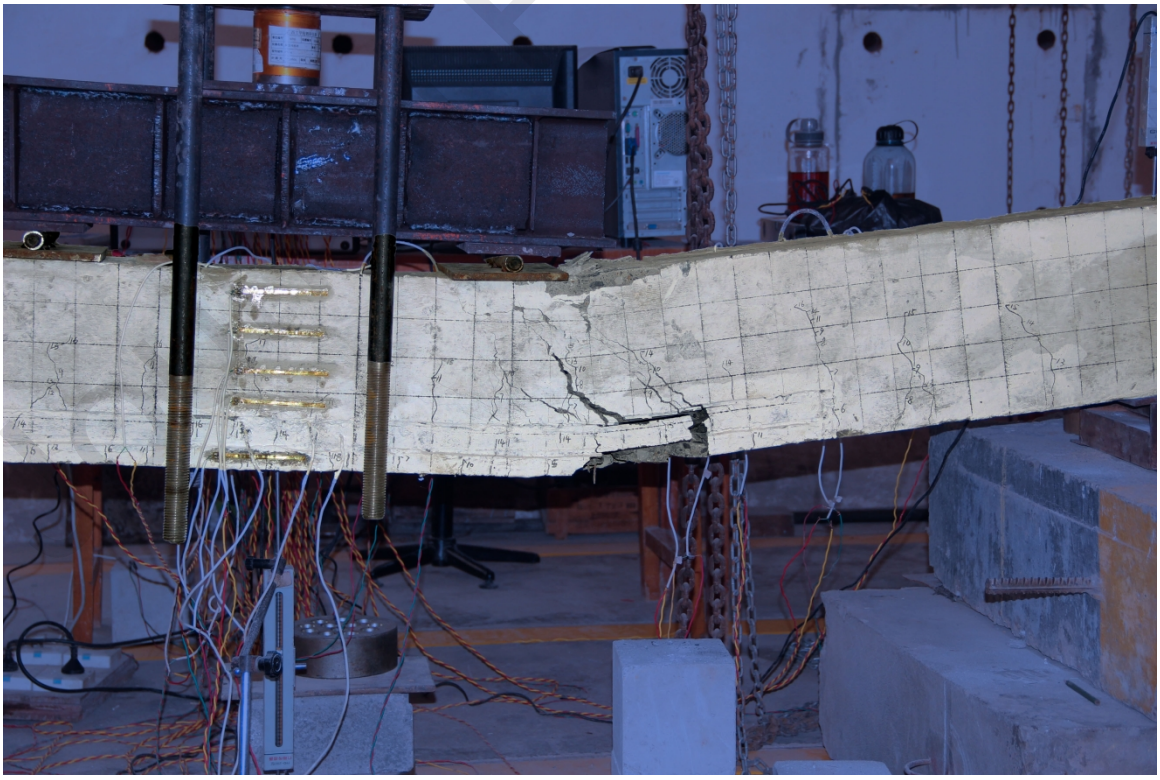

d) Beam JGL4

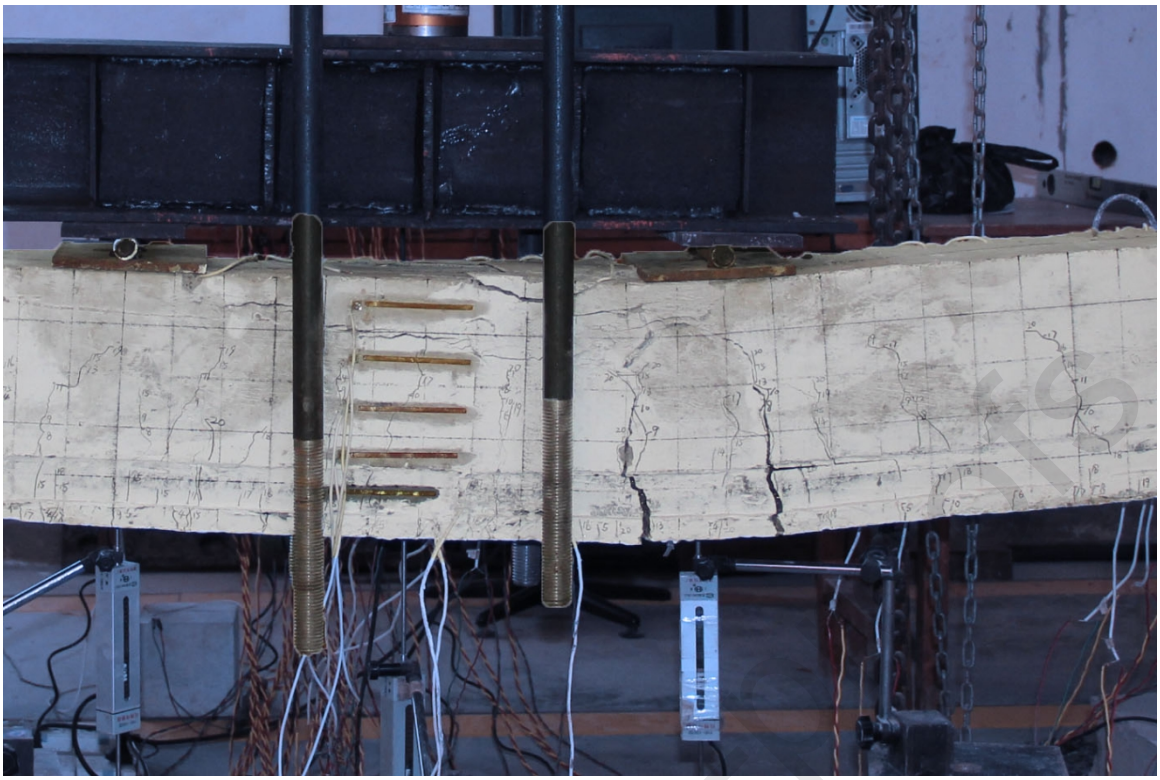

e) Beam JGL5

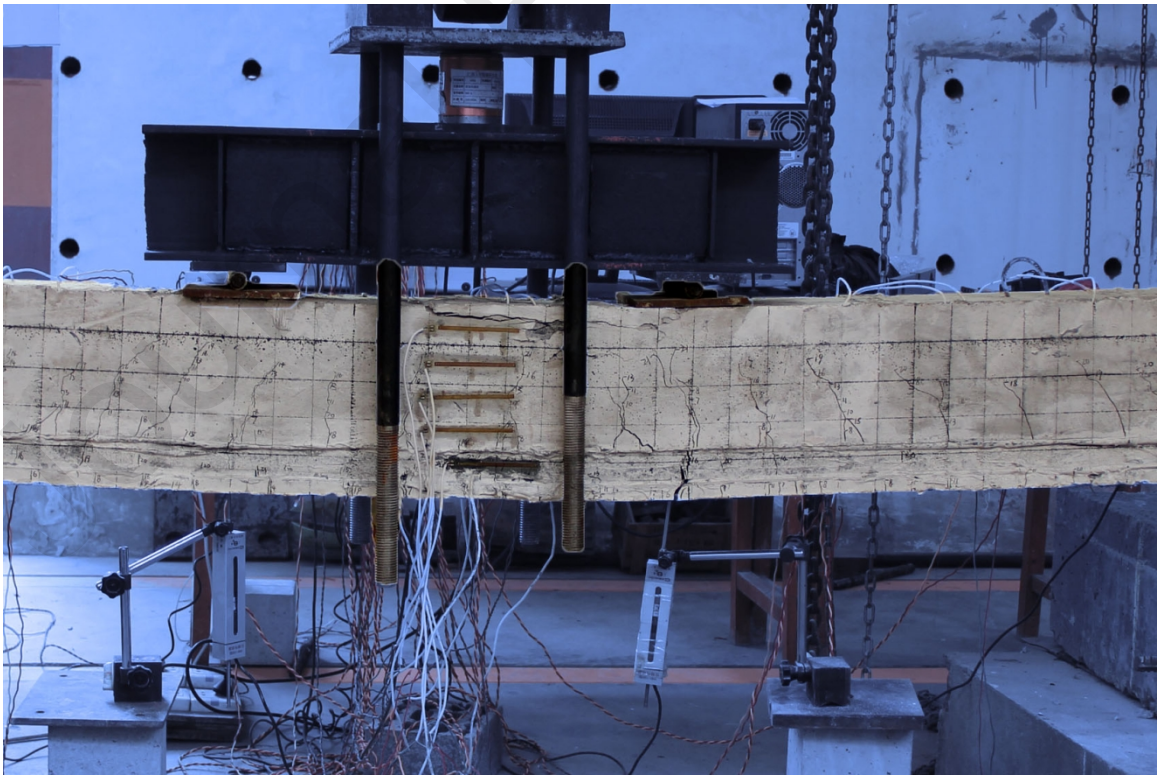

f) Beam JGL6

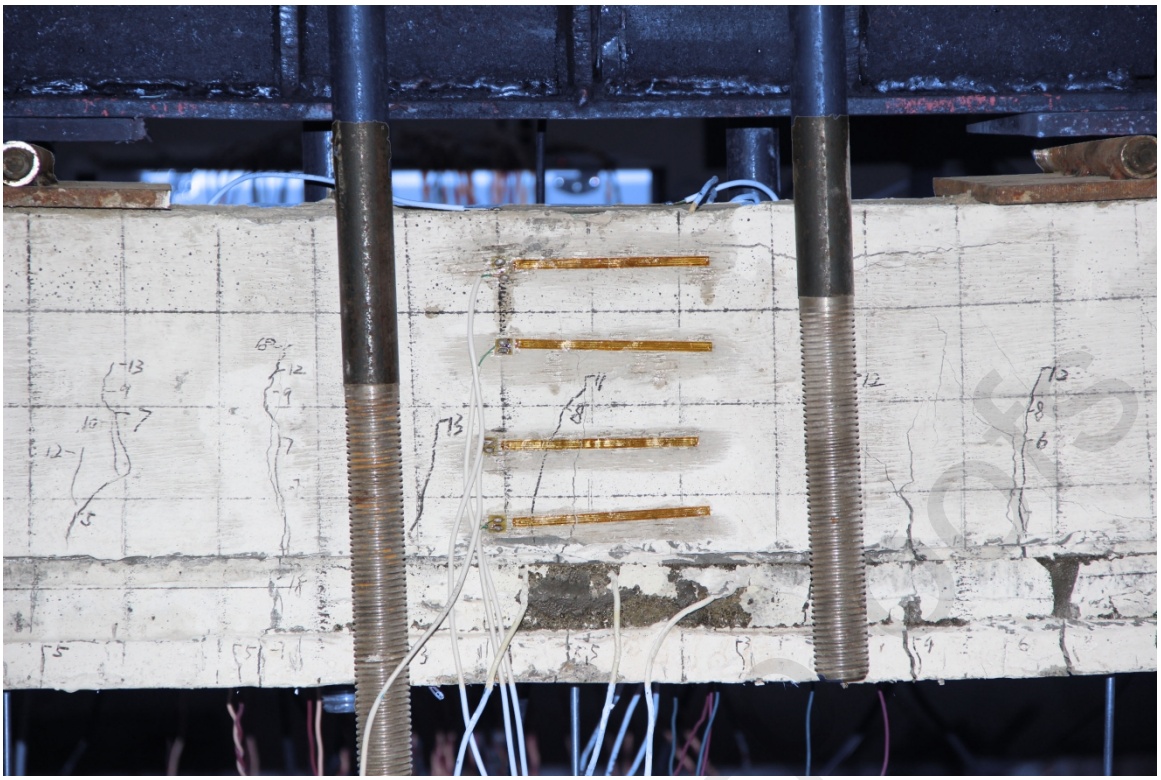

g) Beam JGL7

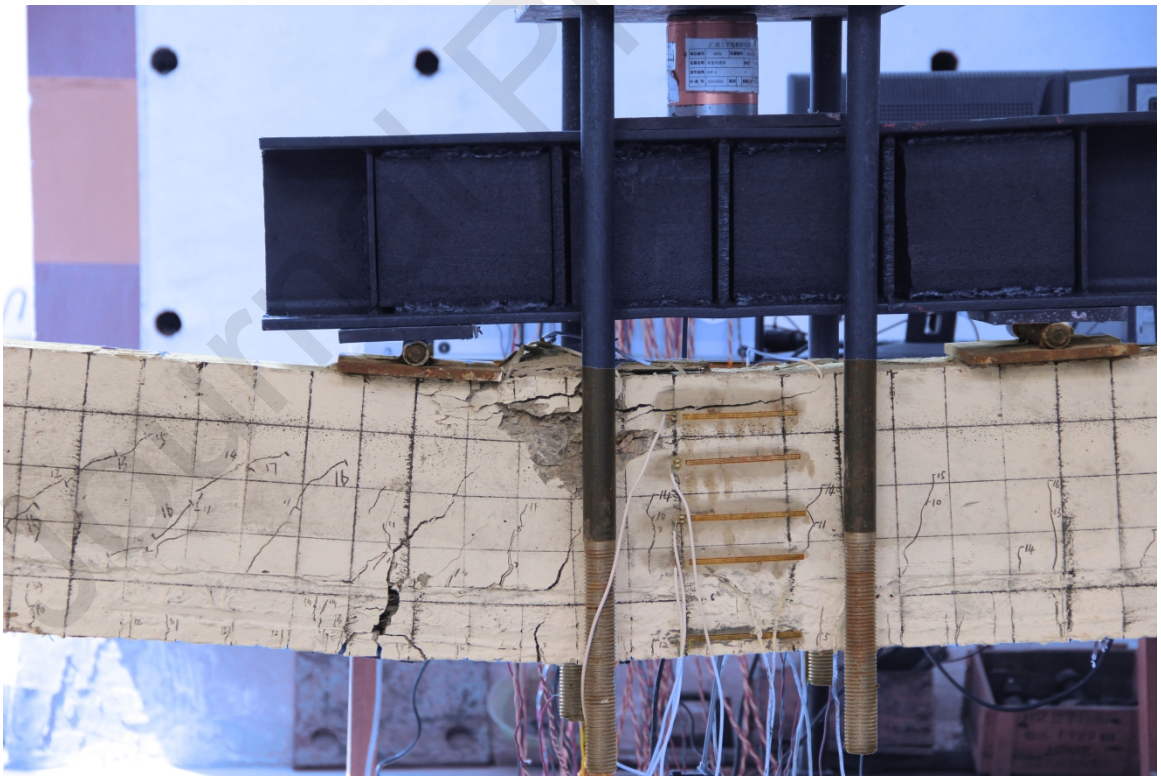

h) Beam JGL8

Fig. 4. Failure modes of the tested beams

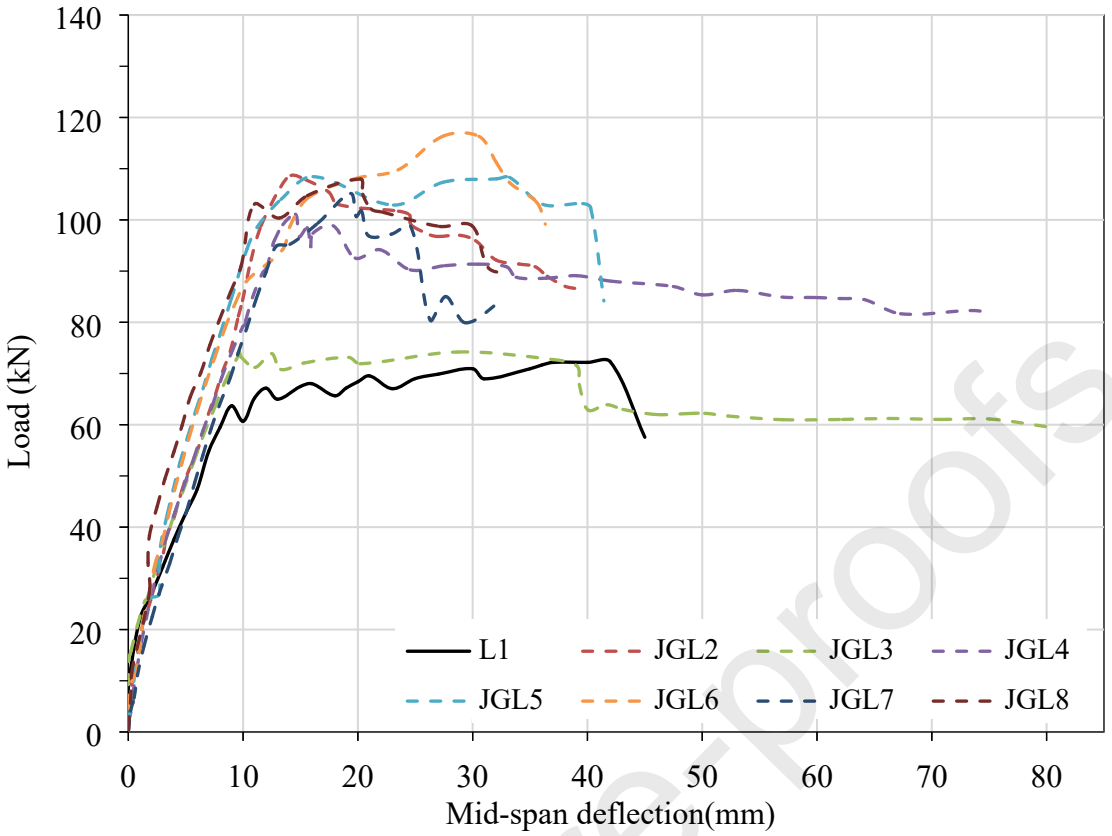

Fig.5. The load-deflection curves of the tested beams

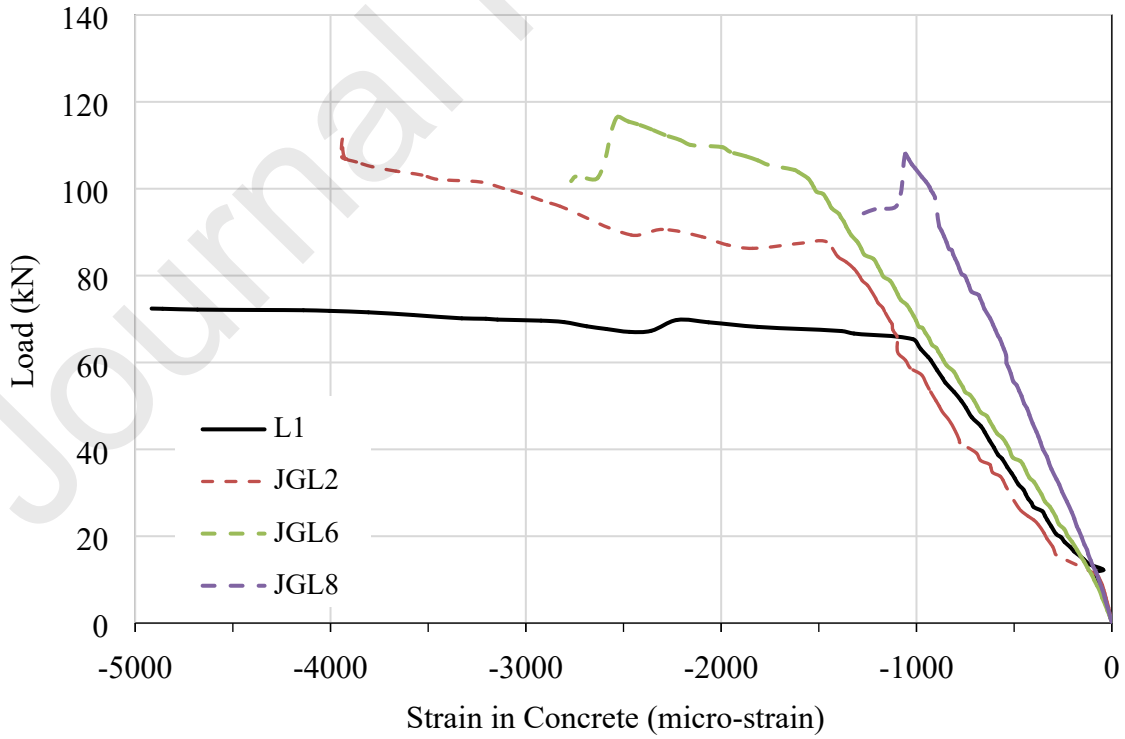

a) Load-strain curve of concrete

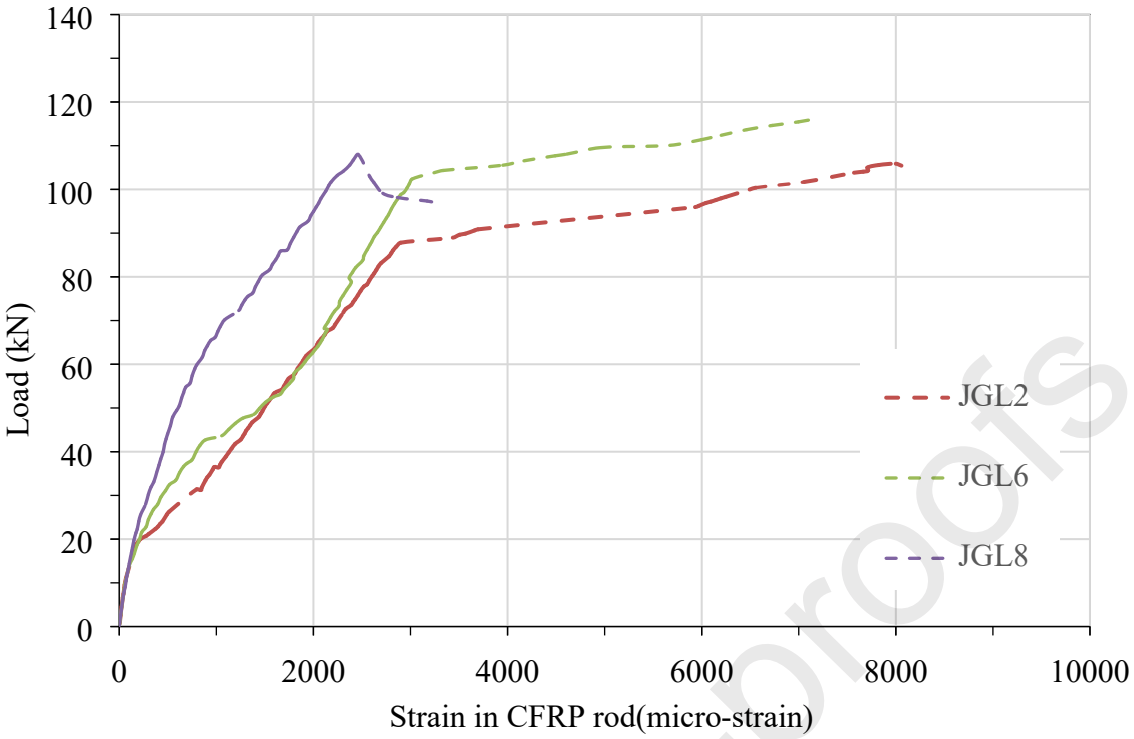

b) Load-strain curve of CFRP rods

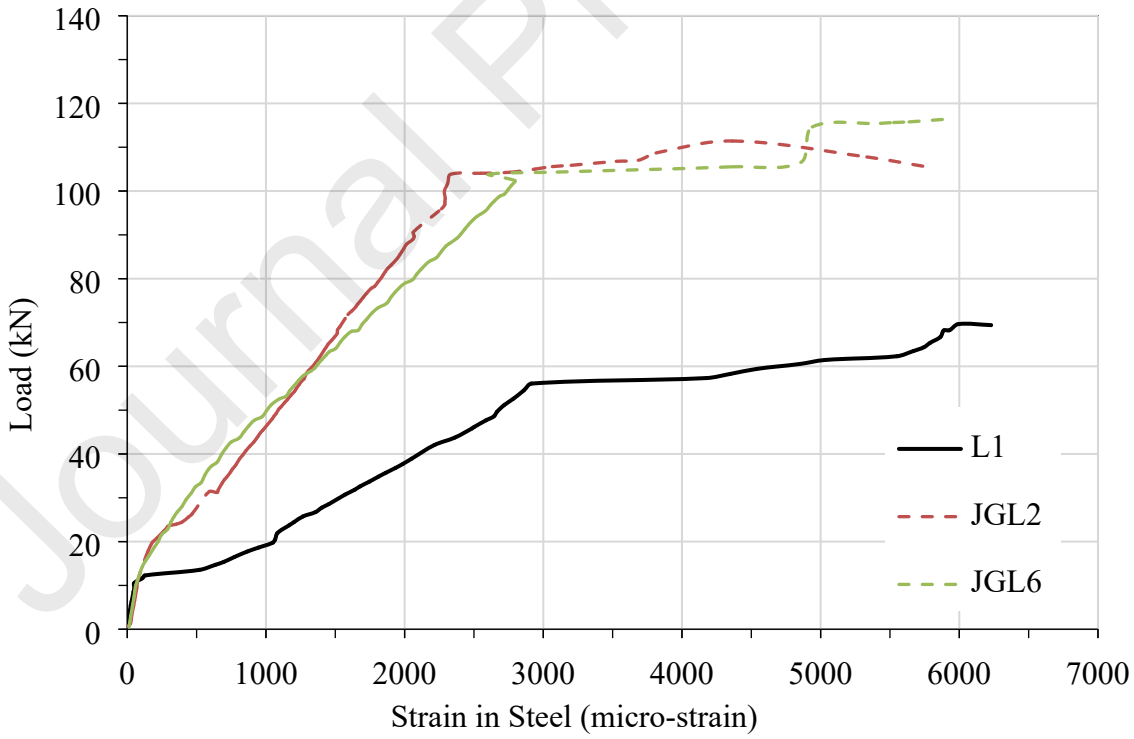

c) Load-strain curve of steel bars in tension

Fig. 6. Load-strain curves of tested beams

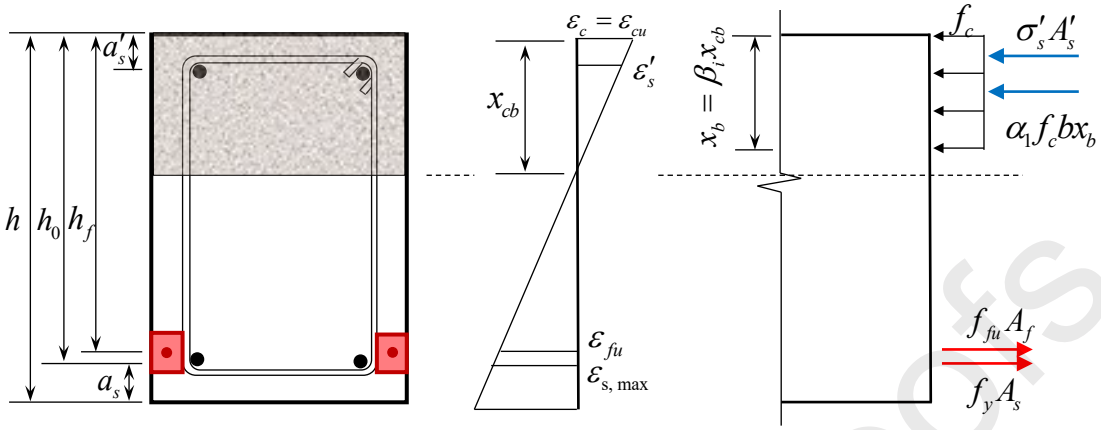

Fig.7 The distribution of strain and stress across a section under the balanced condition

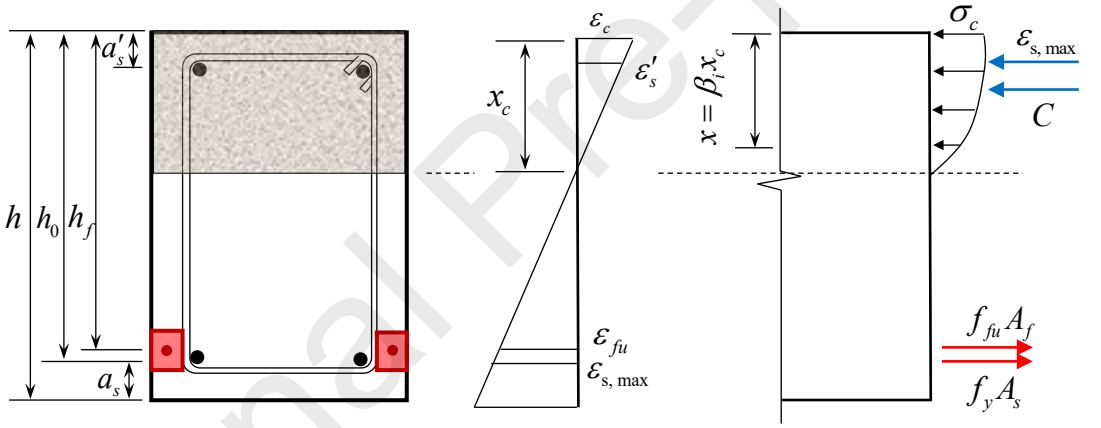

Fig. 8 The distribution of strain and stress across a section under tension failure

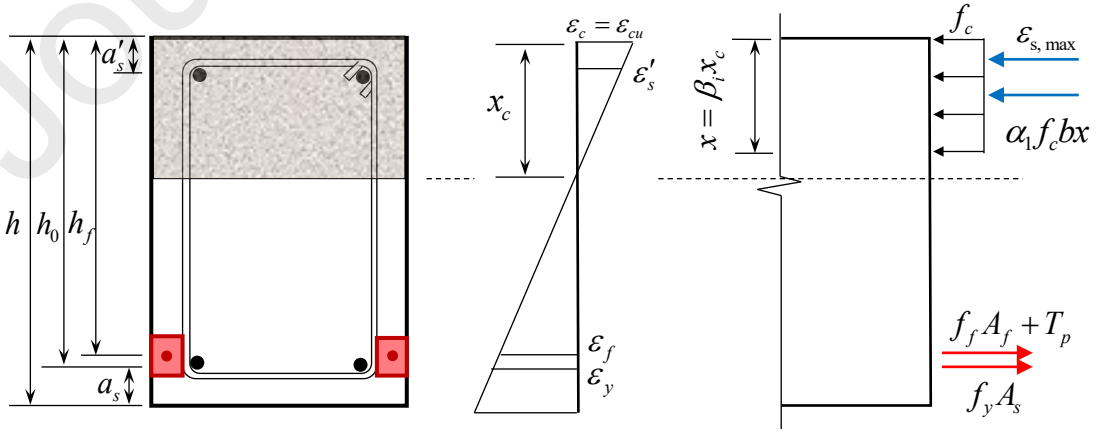

Fig. 9 The distribution of strain and stress across a section under compression failure

Table 1 Parameters of the tested beams

Specimen	Bond length (mm)	Prestress level	Concrete type[a]
L1[b]	-	-	-
JGL2	2200	0%	UHPC
JGL3	1000	30%	UHPC
JGL4	1400	30%	UHPC
JGL5	1800	30%	UHPC
JGL6	2200	30%	UHPC
JGL7	2200	30%	Epoxy resin mortar
JGL8	2200	50%	UHPC

[a] The prisms were cast with ultra-high performance concrete (UHPC) or epoxy resin mortar
[b] Control beam

Table 2 Properties of materials

Materials	Test items	Measured values (MPa)
Concrete	Compressive strength	30.76
	Tensile strength	3.02
	Elastic modulus	3.27×10^4
Steel bars	Yield strength	445
	Ultimate strength	620
	Elastic modulus	2×10^5
UHPC	Compressive strength	154
	Tensile strength	17.4
	Elastic modulus	4.35×10^4
Epoxy resin mortar	Compressive strength	75
	Tensile strength	20
	Elastic modulus	8.5×10^4

Table 3 Main results of test

Specimen	P_{cr} (KN)	P_y (KN)	P_u (KN)	$\delta_u (mm)$	Failure mode
L1	13.18	64.98	69.27	45.2	Bending failure
JGL2	16.47	88.38	108.69	39.2	Bending failure
JGL3	17.96	68.5	74.2	80.08	Debonding failure
JGL4	21.23	89.63	101.02	75.22	Slip failure
JGL5	18.45	91.16	108.45	41.43	Bending failure
JGL6	18.12	104.33	116.36	36.33	Bending failure
JGL7	14.59	94.85	105.15	32.74	Slip failure
JGL8	19.86	91.02	107.97	33.5	Bending failure

Note: P_{cr} is the cracking load of the beams. P_y is the yield load of the beams. P_u is the ultimate load of the beams. δ_u is the ultimate deflection of the beams.

Table 4 Verification of the analytical model for flexural capacity

Specimen	$M_{,exp}$[a] ($KN \cdot m$)	$M_{,ana}$[b] ($KN \cdot m$)	$M_{,exp}/M_{,ana}$
L1	31.17	28.92	1.08
JGL2	48.91	44.51	1.10
JGL3	33.39	35.43	0.94
JGL4	45.46	37.82	1.20
JGL5	48.80	51.07	0.96
JGL6	52.36	53.86	0.97
JGL7	47.32	49.12	0.96
JGL8	48.59	53.00	0.92

[a] The flexural capacity obtained from the experimental studies.
[b] The flexural capacity calculated by the analytical model.

Table 5 Verification of the analytical model for cracking load

Specimen	$P_{cr,exp}$[a] (KN)	$P_{cr,ana}$[b](KN)	$P_{cr,exp}/P_{cr,ana}$
L1	13.18	13.87	0.95
JGL2	16.47	14.87	1.11
JGL3	17.96	19.36	0.93
JGL4	21.23	19.36	1.10
JGL5	18.45	19.36	0.95
JGL6	18.12	19.36	0.94
JGL7	14.59	23.78	0.61
JGL8	19.86	22.79	0.87

[a] The cracking load obtained from the experimental studies.
[b] The cracking load calculated by the analytical model.

Table 6. Verification of the analytical model for deflection.

Specimen	$d_{y,exp}$ [a] (mm)	$d_{y,ana}$ [b](mm)	$d_{,exp}/d_{,ana}$
L1	9.53	8.04	0.84
JGL2	14.62	12.06	0.82
JGL3	9.92	9.34	0.94
JGL4	12.21	10.04	0.82
JGL5	15.24	13.84	0.91
JGL6	15.72	14.59	0.93
JGL7	12.65	13.31	1.05
JGL8	15.03	14.36	0.96

[a] The deflection under the yield load obtained from the experimental studies.
[b] The deflection under the yield load calculated by the analytical model.